Available online at www.sciencedirect.com
SCIENCE DIRECT®
Icarus 179 (2005) 527–534
ICARUS
www.elsevier.com/locate/icarus

Near-infrared laboratory spectra of solid H_2O/CO_2 and CH_3OH/CO_2 ice mixtures

Max P. Bernstein *, Dale P. Cruikshank, Scott A. Sandford

NASA Ames Research Center, MS 245-6, Moffett Field, CA 94035, USA

Received 4 February 2005; revised 6 June 2005

Available online 12 September 2005

Abstract

We present near-IR spectra of solid CO_2 in H_2O and CH_3OH, and find they are significantly different from that of pure solid CO_2. Peaks not present in either pure H_2O or pure CO_2 spectra become evident when the two are mixed. First, the putative theoretically forbidden CO_2 ($2\nu_3$) overtone near 2.134 μm (4685 cm^{-1}), that is absent from our spectrum of pure solid CO_2, is prominent in the spectra of $H_2O/CO_2 = 5$ and 25 mixtures. Second, a 2.74-μm (3650 cm^{-1}) dangling OH feature of H_2O (and a potentially related peak at 1.89 μm) appear in the spectra of CO_2–H_2O ice mixtures, but are probably not diagnostic of the presence of CO_2. Other CO_2 peaks display shifts in position and increased width because of intermolecular interactions with H_2O. Warming causes some peak positions and profiles in the spectrum of a $H_2O/CO_2 = 5$ mixture to take on the appearance of pure CO_2. Absolute strengths for absorptions of CO_2 in solid H_2O are estimated. Similar results are observed for CO_2 in solid CH_3OH. Since the CO_2 ($2\nu_3$) overtone near 2.134 μm (4685 cm^{-1}) is not present in pure CO_2 but prominent in mixtures, it may be a good observational (spectral) indicator of whether solid CO_2 is a pure material or intimately mixed with other molecules. These observations may be applicable to Mars polar caps as well as outer Solar System bodies.
Published by Elsevier Inc.

Keywords: Ices, infrared observations; Spectroscopy; Surfaces, planets, satellites

1. Introduction

Near-infrared (IR) reflection spectra of outer Solar System objects show that CO_2 occurs on the solid surfaces of several bodies in the Solar System. In addition to the seasonal deposits of solid CO_2 on Mars, carbon dioxide in the comae of some comets is presumed to evaporate from solid CO_2 in their nuclei; comets also contain CH_3OH (Mumma et al., 1993). Grundy et al. (2003) found three bands of solid CO_2 in the 2-μm region in the spectrum of the uranian satellite Ariel. Carbon dioxide is also seen in the reflectance spectra of Jupiter's satellites Europa, Ganymede, and Callisto (McCord et al., 1997, 1998; Hibbits et al., 2000, 2003) and Saturn's satellites Phoebe (Clark et al., 2005) and Iapetus (Buratti et al., 2005). In all of these cases, the CO_2 stretching fundamental band usually at 4.27 μm is shifted slightly to shorter wavelength (4.26 μm) and is presumed to originate from CO_2 that is complexed in some way with other surface materials. The occurrence of CO_2 in the form of fluid or gaseous inclusions in minerals has been suggested by the authors of the papers cited above.

On Triton, an environment that is dominated by N_2 (Cruikshank et al., 1993; Stansberry, 2004), CO_2 might have been frozen into an inert matrix of solid N_2, but lab experiments have shown that the IR absorptions (especially the $4\nu_2 + \nu_3$ band) are more consistent with pure CO_2 (Quirico et al., 1999) than CO_2 in N_2 (Quirico and Schmitt, 1997). Even if they were originally mixed, presumably seasonal temperature cycling and surface–atmosphere exchange has caused the ice components to separate on Triton and Pluto (e.g., Grundy and Buie, 2001) and on Mars (Bibring et al., 2004). The IR spectrum of pure solid CO_2 has been

* Corresponding author.
E-mail address: mbernstein@mail.arc.nasa.gov (M.P. Bernstein).

0019-1035/$ – see front matter Published by Elsevier Inc.
doi:10.1016/j.icarus.2005.07.009

well studied (Hansen, 1997; Quirico and Schmitt, 1997; Gerakines et al., 2005) and modeled (Bini et al., 1991), so it is well understood.

Solid H_2O is ubiquitous in the outer Solar System (Roush, 2001), and it is inevitable that CO_2 will come into intimate contact with H_2O at various temperatures and in varied proportions. For example, reflectance spectra of icy Galilean and saturnian satellites show strong near-IR absorptions of H_2O and CO_2. Although good near-IR spectra of pure CO_2 and CO_2 in N_2 have been published (Hansen, 1997; Quirico and Schmitt, 1997; Gerakines et al., 2005), to our knowledge no near-IR spectra of CO_2 in H_2O are available. The interaction between CO_2 and H_2O (and CH_3OH) on a molecular level has been shown to cause significant changes in the position and profile of CO_2 peaks in the mid-IR (Sandford and Allamandola, 1990; Dartois et al., 1999; Ehrenfreund et al., 1999; Palumbo and Baratta, 2000), so it seems reasonable that the presence of H_2O could change near-IR CO_2 peaks as well. Indeed, in this paper we show that this is the case, especially for the classically 'forbidden' $2\nu_3$ overtone near 2.134 μm.

The coincidence of CO_2 and CH_3OH in spectra of comets shows that these molecules coexist in the ices of the nucleus, but it is unknown if they occur as a molecular mix or in some other configuration. Both CH_3OH and H_2O ices have been found on the Centaur object 5145 Pholus (Cruikshank et al., 1998), thought to be a former Kuiper belt object and therefore a large 'proto-comet,' but CO_2 has not yet been detected.

In this paper we display near-IR spectra of H_2O–CO_2 and CH_3OH–CO_2 ice mixtures at temperatures from 15 to 150 K. Among other things we highlight the enhancement of the probable $2\nu_3$ overtone of CO_2 near 2.134 μm (4685 cm^{-1}), and its potential as an observational (spectral) indicator of whether solid CO_2 is a pure material or intimately mixed with other molecules. We present these results in Section 3, and briefly discuss the results and potential implications for Solar System studies in Section 4.

2. Materials and methods

The basic techniques and equipment employed for this study have been described previously as part of our mid-IR studies of various compounds in H_2O at low temperature (Hudgins et al., 1994). Details associated with the materials and methods used that are unique to this particular study are provided below.

The H_2O (purified via a Millipore Milli-Q water system to 18.2 MΩ) and the CH_3OH (99.93% HPLC grade, Aldrich) were freeze-pump thawed at least three times to remove dissolved gases prior to use. CO_2 (bone dry, Matheson) was used without further purification. Samples were mixed at room temperature in volume-calibrated, greaseless glass bulbs and allowed to equilibrate for at least 24 h before use. The background pressure in the gas-handling system was $\sim 10^{-5}$ mbar, compared to total pressures in the sample bulbs of tens of millibars, so the contaminant levels in the bulbs associated with the mixing process were negligible. Bulbs containing $H_2O/CO_2 = 5$ and 25, and $CH_3OH/CO_2 = 5$ mixtures were used to prepare the samples.

Once prepared, glass sample bulbs were transferred to the stainless steel vacuum manifold where the sample mixture was vapor-deposited onto a CsI window cooled to 15 K by an Air Products Displex CSW 202 closed-cycle helium refrigerator. Gas mixtures were deposited first for 10 min against a cold shield before depositing onto the sample window so as to minimize the bias in the ice towards the more volatile component early in the deposit. We find that this procedure gives a solid sample more representative of the gas phase mixing ratio in the bulb, but presumably also depends on the components and the substrate temperature.

Typical samples were deposited at a rate sufficient to produce samples ∼0.1 μm thick after a few minutes. The spectra that include the mid-IR (Figs. 1 and 7) are only tenths of micrometers thick, whereas the others are ∼10 μm thick. Under these conditions the samples are composed of an intimate mixture of the CO_2 in H_2O or CH_3OH. Pure H_2O deposited under these conditions is in its high density amorphous form when deposited at 15 K and after warming, the H_2O goes through several phase transitions (Jenniskens and Blake, 1994; Jenniskens et al., 1995). Clearly, the situation for mixtures is more complex. We do not know the phase of the H_2O in these mixtures but our IR spectra of H_2O/CO_2 mixtures are broadly consistent with previous observations of phases of pure H_2O.

In Table 1, we report relative areas for the absorptions of CO_2 in H_2O and CH_3OH because we have no accurate absolute scale against which to compare the peak areas. However, we can give an estimate of the intrinsic (absolute) absorptivities for these absorptions of CO_2 in solid H_2O given certain assumptions. If we assume that the intrinsic strength of the 4.270 μm (2342 cm^{-1}) ν_3, fundamental asymmetric stretch of CO_2 in the spectrum of the $H_2O/CO_2 = 25$ ice is the same as that of an $H_2O/CO_2 = 20$ mixture, then it should be $\sim 2 \times 10^{-16}$ cm/molec according to Sandford and Allamandola (1990). Since the numbers on Table 1 are normalized to the ν_3 band, the relative numbers in Table 1 (at least for the $H_2O/CO_2 = 25$ ice) can be converted to intrinsic per-molecule absorptivities (A values) by multiplying by $\sim 2 \times 10^{-16}$ cm/molec.

The intensity of the 2.135 μm (4700 cm^{-1}) 'forbidden' $2\nu_3$ overtone of CO_2 in H_2O or CH_3OH is sensitive to conditions (i.e., concentration, temperature); we have observed it to vary in strength by as much as a factor of two in CO_2–CH_3OH mixtures. As a result, the areas reported for the 2.135 μm (4700 cm^{-1}) absorptions should be regarded as more uncertain than those of the other CO_2 absorptions.

Table 1
Peak areas for solid CO_2 in H_2O and CH_3OH at 15 K

Mode[a]	$H_2O/CO_2 = 25$			$H_2O/CO_2 = 5$			$CH_3OH/CO_2 = 5$		
	Position (cm^{-1})	FWHM (cm^{-1})	Area[b]	Position (cm^{-1})	FWHM (cm^{-1})	Area[b]	Position (cm^{-1})	FWHM (cm^{-1})	Area[b]
$2\nu_1 + \nu_3$	–	–	–	5083	10	6.3×10^{-5}	5071	18	1.2×10^{-4}
$\nu_1 + 2\nu_2 + \nu_3$	4960	>10	$\sim 6 \times 10^{-4}$	4962	15	1.7×10^{-4}	4950	14	1.8×10^{-4}
$4\nu_2 + \nu_3$	–	–	–	4827	–	1.1×10^{-5}	4847	–	$\sim 1 \times 10^{-5}$
$2\nu_3$	4685	27	0.012	4678	40	0.016	4680	20	0.015
$\nu_1 + \nu_3$	3700	12	0.013	3702	12	8.4×10^{-3}	3697	11	0.014
–	3650[c]	20	6.4×10^{-3}	3653[c]	32	0.048	3627[c]	16	0.0022
$2\nu_2 + \nu_3$	–	–	–	3592	11	1.3×10^{-3}[d]	3584	15	3.6×10^{-3}
ν_3	2342	11	1.0	2341	22	1.0	2339	18	1.0
$^{13}C-\nu_3$	2278	8	0.010	2279	8	0.010	2275	6	0.010
ν_2	653	21	0.15	654	20	0.21	646	31	0.18

[a] Mode assignments from Quirico and Schmitt (1997) and Sandford and Allamandola (1990).
[b] Peak areas are normalized to the CO_2 peak near 2340 cm^{-1} (4.274 μm). The relative numbers can be converted to absolute values by multiplying by $\sim 2 \times 10^{-16}$ cm/molec (see Section 2).
[c] These are not CO_2 peaks, they are probably caused by H_2O (or CH_3OH).
[d] This area probably represents a lower limit, this peak is difficult to integrate accurately because of its proximity to the 3 μm OH band of H_2O.

3. Results

Fig. 1 displays a full (1.75–22 μm; 5700–450 cm^{-1}) IR spectrum of an $H_2O/CO_2 = 5$ mixture at 15 K. The broad strong absorptions at ~2.0, 3.1, 6.3, and 13.3 μm (5090, 3250, 1600, and 750 cm^{-1}) are typical of those observed previously for pure amorphous solid H_2O (Hudgins et al., 1994; Gerakines et al., 2005). Solid H_2O is also responsible for the sharper, weaker, features near 1.89 μm (5300 cm^{-1}) and 2.74 μm (3650 cm^{-1}), see discussion for details. The sharp mid-IR peaks of CO_2 in solid H_2O appear at 15.3 μm (654 cm^{-1}), 4.39 μm (2278 cm^{-1}), and 4.270 μm (2342 cm^{-1}), and these have been well studied (Sandford and Allamandola, 1990; Dartois et al., 1999). The shorter wavelength, less intense, (near) IR absorptions of CO_2 in solid H_2O are at 2.701, 2.784, 2.135, 2.072, 2.015, and 1.967 μm (3592, 3702, 4678, 4827, 4962, and 5083 cm^{-1}). Table 1 lists the peak positions, full widths at half maximum height (FWHM) and relative areas of all observed absorptions of CO_2.

The CO_2 absorption at 4.270 μm (2342 cm^{-1}) that dominates the mid-IR and Fig. 1 corresponds to ν_3, the asymmetric stretch of CO_2. We believe that the peak at 2.135 μm (4684 cm^{-1}) is $2\nu_3$, the theoretically 'forbidden' first overtone of the asymmetric stretch of CO_2 (see inset in Fig. 1). Because we have not performed isotopic studies, this assignment is based merely on the fact that it appears at twice the frequency of ν_3 and behaves in a manner consistent with it being a 'forbidden' feature, i.e., this peak is absent from or very much weaker in spectra of pure solid CO_2 (see below).

Below we present a series of figures highlighting spectral regions of particular interest. The figures in this paper show primarily spectra of $H_2O/CO_2 = 5$ mixtures because these display the CO_2 absorptions with better signal-to-noise, but the positions and widths are representative of what is seen for $H_2O/CO_2 = 25$ (see table for details).

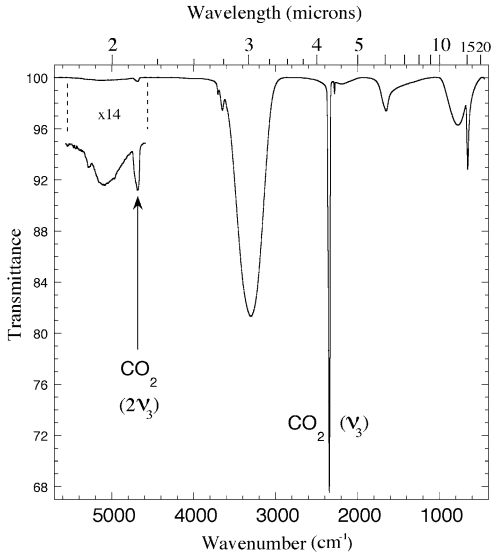

Fig. 1. The 1.75–22 μm (5700–450 cm^{-1}) IR spectrum of an $H_2O/CO_2 = 5$ ice mixture at 15 K. In addition to the broad absorptions of amorphous solid H_2O and the sharper CO_2 fundamentals one sees the 'forbidden' $2\nu_3$ overtone of CO_2 at 2.135 μm (4684 cm^{-1}). This feature is prominent in spectra of mixtures but is not seen in spectra of pure CO_2 (see Fig. 3).

Fig. 2 shows 2.667–2.817 μm (3750–3550 cm^{-1}) IR spectrum of pure CO_2 (top trace) compared with that of an $H_2O/CO_2 = 5$ ice mixture at 15 K. The two peaks at 2.701 and 2.784 μm (3702 and 3592 cm^{-1}) can be attributed to the $\nu_1 + \nu_3$ and $2\nu_2 + \nu_3$ combination modes of CO_2, respectively (Sandford and Allamandola, 1990; Quirico and Schmitt, 1997).

These absorptions of CO_2 in solid H_2O are 4–5 times broader and shifted by 0.005 and 0.006 μm (−7 and −8 cm^{-1}), respectively, relative to pure solid CO_2 under the same conditions. The central broad absorption near 2.74 μm

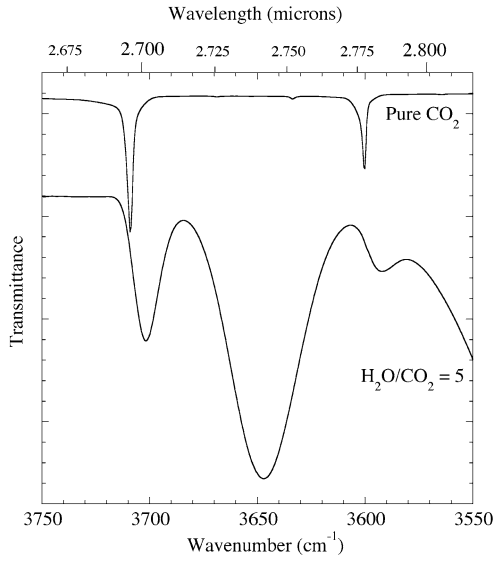

Fig. 2. The 2.667–2.817 μm (3750–3550 cm^{-1}) IR spectrum of pure CO_2 (above) compared with that of an $H_2O/CO_2 = 5$ ice mixture at 15 K (below). The ∼2.70 and 2.78 μm (3702 and 3592 cm^{-1}) absorptions of CO_2 in H_2O are significantly broader and shifted to longer wavelength than those of pure CO_2. The central broad feature near 2.74 μm (3650 cm^{-1}) is an absorption of H_2O, not CO_2, so it does not appear in the upper spectrum. The lower spectrum drops off to the right because of the large 3 μm H_2O band (see Fig. 1).

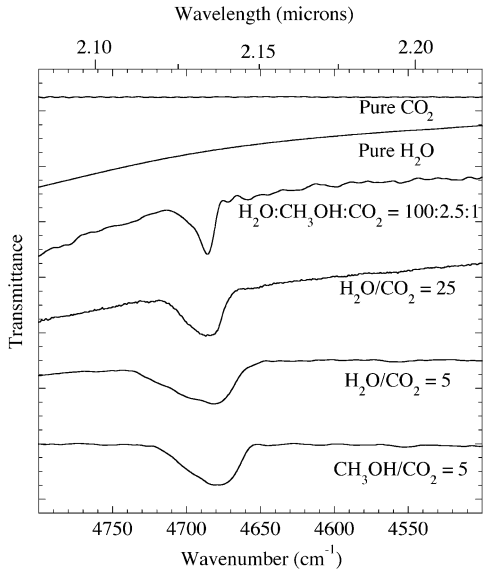

Fig. 3. The 2.08–2.27 μm (4800–4400 cm^{-1}) IR spectra of pure CO_2 and H_2O compared with those of various H_2O, CH_3OH, and CO_2 containing ice mixtures at 15 K. The $2\nu_3$ overtone of the asymmetric stretch of CO_2 near 2.135 μm (4684 cm^{-1}) is absent from the spectra of pure CO_2 and pure H_2O, but present in the spectra of the CO_2 mixed with H_2O and/or CH_3OH. The position and profile of this overtone is sensitive to ice composition and concentration, not unusual behavior for a classically 'forbidden' feature. The baselines of the spectra rich H_2O in drop off to the left because of the 2 μm H_2O band (see Fig. 1).

(3650 cm^{-1}) is very similar to that assigned by Rowland et al. (1991) to the 'dangling' OH of H_2O and discussed in an astrophysical context by Ehrenfreund et al. (1996). This feature is observed when any molecule mixed into solid H_2O breaks up its hydrogen bonding network. Thus, it is not specific to CO_2.

Fig. 3 highlights the $2\nu_3$ 'forbidden' overtone of CO_2 at 2.135 μm (4684 cm^{-1}) previously seen in the inset in Fig. 1. In this figure the 2.08–2.27 μm (4800–4400 cm^{-1}) IR spectra of $H_2O/CO_2 = 5$ and $= 25$, $CH_3OH/CO_2 = 5$, and H_2O:CH_3OH:CO_2 =100:2.5:1 mixtures are compared to those of pure CO_2 and pure H_2O under the same conditions. The $2\nu_3$ overtone of the asymmetric stretch of CO_2 near 2.135 μm (4684 cm^{-1}) is present in all of the ice mixtures, but it is too weak to be observed in the spectrum of pure CO_2 (above), although there are at least 100 times more CO_2 molecules in the sample that produced the upper trace than in the lower ones.

There are three sharp peaks in the spectrum of pure CO_2 at 2.072, 2.015, and 1.967 μm (4827, 4962, and 5083 cm^{-1}) (Hansen, 1997; Quirico and Schmitt, 1997; Gerakines et al., 2005), as can be seen in the upper trace in Fig. 4. Compared to pure CO_2 these absorptions from the mixture are 3–5 times broader and shifted to longer wavelength by 0.002, 0.004, and 0.003 μm (6, 10, and 5 cm^{-1}), respectively. This is comparable to the broadening and shifting of the 2.70 and 2.78 μm (3702 and 3593 cm^{-1}) CO_2 peaks in Fig. 2. This entire region of the spectrum is spanned by a broad H_2O band (see also Fig. 1), and this causes a broad dip in the spectra of H_2O–CO_2 mixtures that somewhat obscures these CO_2 peaks.

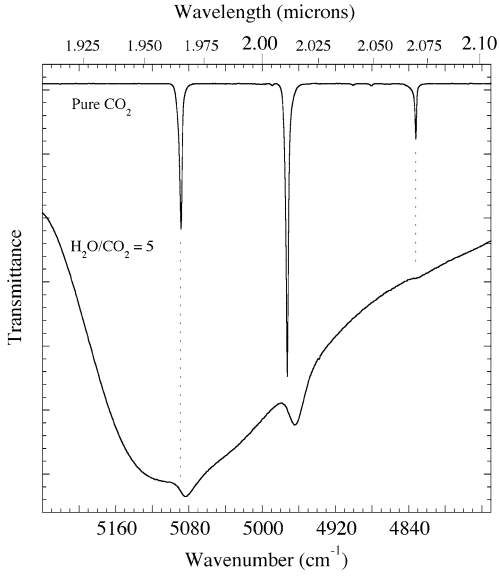

Fig. 4. The 1.908–2.105 μm (5240–4750 cm^{-1}) IR spectrum of pure CO_2 (above) compared with that of an $H_2O/CO_2 = 5$ ice mixture (below) at 15 K. The large broad dip crossing the entire lower trace is caused by H_2O. The smaller peaks at ∼1.97, 2.01, and 2.07 μm (5083, 4963, and 4827 cm^{-1}) are from CO_2 in H_2O. Compared to pure CO_2 these absorptions from the mixture are significantly broader and shifted to longer wavelength.

Fig. 5 shows the temperature dependence of the 2.70 and 2.78 μm (3702 and 3593 cm^{-1}) absorptions of a $H_2O/CO_2 = 5$ ice between 15 and 100 K. Sharp peaks con-

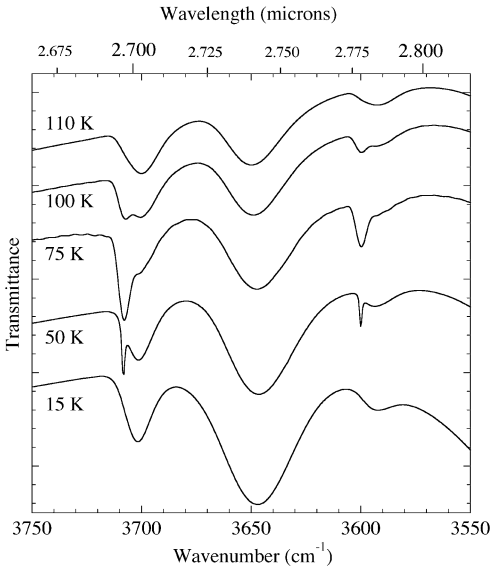

Fig. 5. Temperature dependence of the 2.67–2.82 μm (3750–3550 cm^{-1}) IR spectrum of an $H_2O/CO_2 = 5$ ice mixture. The broad features at ~2.70 and 2.79 μm (3700 and 3590 cm^{-1}) of CO_2 in H_2O are visible over the entire temperature range. The sharper peaks superimposed upon them that appear, broaden, and then diminish with warming are similar to those produced by pure CO_2.

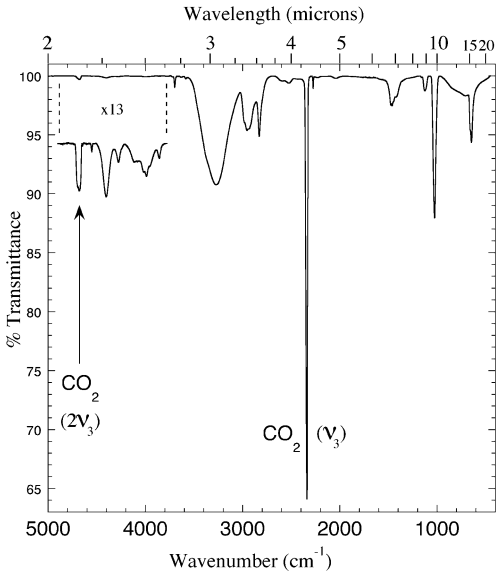

Fig. 6. The 2.0–22 μm (5000–450 cm^{-1}) IR spectrum of an $CH_3OH/CO_2 = 5$ ice mixture. As in Figs. 1 and 3, the $2\nu_3$ overtone of CO_2 is clearly visible at ~2.14 μm (4682 cm^{-1}), and the pair of CO_2 peaks at ~2.70 and 2.79 μm are also present. The other absorptions between 2 and 3 μm are caused by methanol.

sistent with pure CO_2 are superimposed on the broader absorptions typical of CO_2 in H_2O (compare Fig. 5 to Fig. 2). Since the latter are visible over the entire temperature range, but the sharper peaks upon them broaden and diminish with warming, we assume this corresponds to the regions of pure CO_2 forming and then subliming away with rising temperature. Spectra of other CO_2 peaks and the $H_2O/CO_2 = 25$ mixture tell the same story. Blake et al. (1991) and Ehrenfreund et al. (1999) observed similar effects in the mid-IR spectra of CO_2–H_2O–CH_3OH ternary mixtures and attributed it to phase separation and ice 'segregation,' respectively. Our observations of the effects of warming CO_2 in H_2O and CH_3OH (see below) are consistent with those previous observations. The fact that the broader peaks assigned to CO_2 in H_2O remain to well over 100 K reminds us that CO_2 in H_2O will remain observable in the solid phase to much higher temperature than it would in the pure state (Sandford and Allamandola, 1990).

Our observations for a $CH_3OH/CO_2 = 5$ ice mixture are very similar to those described above for $H_2O/CO_2 = 5$. Our spectra are consistent with previously published mid-IR spectra of CO_2 in the presence of CH_3OH (Dartois et al., 1999; Ehrenfreund et al., 1999; Palumbo and Baratta, 2000). Although the 2–2.75 μm (5000–3636 cm^{-1}) spectrum of CH_3OH is more complicated than that of H_2O, the CO_2 features seen in Fig. 6 are similar to those seen in Fig. 1. As before, the pair of CO_2 peaks near 2.70 and 2.79 μm are present, and the putative $2\nu_3$ overtone of CO_2 is clearly visible at ~2.137 μm (4680 cm^{-1}). The intensity of the 2.137 μm (4680 cm^{-1}) peak relative to the fundamental at 4.27 μm (2340 cm^{-1}), is similar to that seen for the $H_2O/CO_2 = 5$ mixture (see Table 1). As with H_2O/CO_2 mixtures the intensity of this ~2.13 μm peak of CO_2 in CH_3OH is sensitive to conditions (i.e., concentration, temperature); we have observed it to vary as much as a factor of two in CO_2–CH_3OH mixtures. As a result the areas reported for the 2.13 μm (4700 cm^{-1}) 'forbidden' $2\nu_3$ absorption should be should be regarded as more uncertain than the other CO_2 absorptions.

As above, the changes in the spectrum of the $CH_3OH/CO_2 = 5$ ice with warming are consistent with ice 'segregation.' Fig. 7 shows the temperature dependence of the IR spectrum of a $CH_3OH/CO_2 = 5$ ice mixture in three regions: between 2.041–2.198 μm (4900–4550 cm^{-1}), 2.667–2.817 μm (3750–3550 cm^{-1}), and 4.167–4.386 μm (2400–2280 cm^{-1}). The 2.13 μm (4700 cm^{-1}) $2\nu_3$ overtone (at left) displays multiple components roughly matching those of the 4.27 μm (2340 cm^{-1}) ν_3 fundamental (right). Similar spectra of the 4.27 μm (2340 cm^{-1}) peak of CO_2 in an H_2O–CH_3OH mixture were published by Blake et al. (1991). The 2.7 and 2.78 μm (3700 and 3600 cm^{-1}) absorptions with broad profiles at 15 K indicative of CO_2 in CH_3OH give way to the sharper peaks resembling pure CO_2 on warming. At 130 K the 2.7 and 2.78 μm (3700 and 3600 cm^{-1}) absorptions look like those of pure CO_2. It cannot be pure CO_2, however, because this would have sublimed away in our vacuum system.

4. Discussion

We have shown that near-IR spectra of CO_2 in H_2O or CH_3OH at low temperature look very different than those pure CO_2 under the same conditions. First, absorptions of

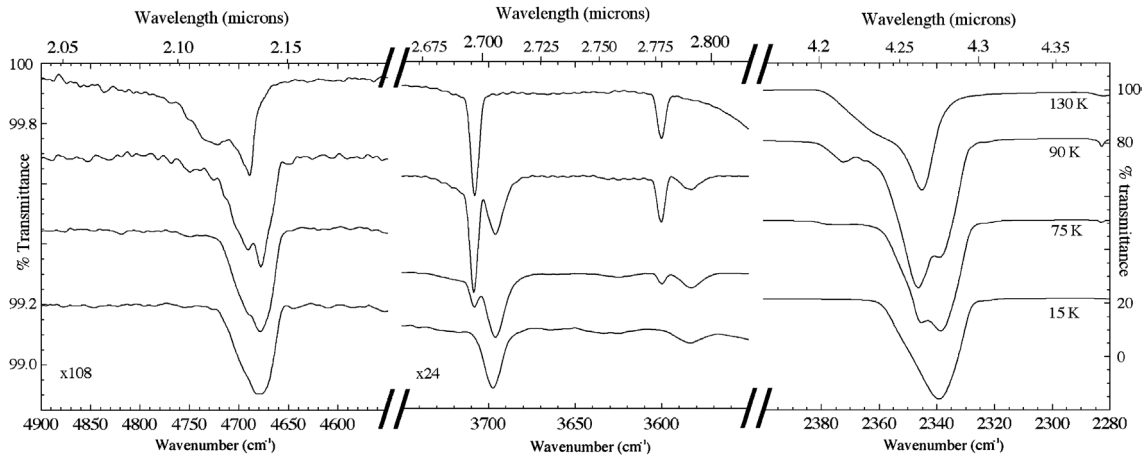

Fig. 7. Temperature dependence of the IR spectrum of a $CH_3OH/CO_2 = 5$ ice mixture between 2.041–2.198 μm (4900–4550 cm^{-1}), 2.667–2.817 μm (3750–3550 cm^{-1}), and 4.167–4.386 μm (2400–2280 cm^{-1}). The $2\nu_3$ overtone (left) near 2.13 μm (4700 cm^{-1}) displays multiple components roughly matching those of the ν_3 fundamental (right) near 4.27 μm (2340 cm^{-1}). The combination modes (center) near 2.7 and 2.78 μm (3700 and 3600 cm^{-1}) have broad profiles at 15 K that give way on warming to sharper peaks resembling those of pure CO_2. However, pure CO_2 would have sublimed by 130 K.

CO_2 in H_2O or CH_3OH are 3–5 times broader and are shifted to longer wavelength by 0.002–0.006 μm (−5 and −10 cm^{-1}) than those of pure CO_2 under the same conditions. Second, and perhaps most significantly, CO_2 in H_2O (or CH_3OH) produces new absorptions that are simply not present (or greatly diminished) in the spectra of the pure materials.

In particular, our near-IR spectra of 1 and 10 μm thick $H_2O/CO_2 = 5$ and 25 ices show a fairly strong ($\sim 10^{-18}$ cm/molec) peak near 2.135 μm (4684 cm^{-1}) interpreted to be the $2\nu_3$ overtone of CO_2 that is very much weaker in near-IR spectra of our pure CO_2 frost (see Fig. 3) and absent from spectra of a thick CO_2 monocrystal grown in a closed cell (E. Quirico, private communication). A very weak peak near ∼2.128 μm (4700 cm^{-1}) was observed in the published spectrum of a thick sample of pure CO_2 (Quirico and Schmitt, 1997) and both they and we think this is the same feature. They observed that small feature to be >7000 times weaker than the 2.70 μm (3700 cm^{-1}) CO_2 peak, whereas these two are of comparable intensity in our spectra of H_2O–CO_2 mixtures (see Table 1). This indicates that the CO_2 $2\nu_3$ absorption is enhanced by a factor of $\sim 10^4$ in our H_2O–CO_2 mixtures, over that of pure CO_2. This formally 'forbidden' absorption has also been reported as a weak feature in the spectra of CO_2 isolated in Ar (Sandford et al., 1991) and N_2 matrices (Quirico and Schmitt, 1997), where we estimate it is at least 1000 times less intense than in H_2O or CH_3OH. The fact that this forbidden transition is observed so strongly suggested that the symmetry of the CO_2 is broken by interactions with neighboring molecules—literally being bent by the water 'matrix' for example. However, were this the case then one might expect that the ν_1 mode near 7.5 μm (1340 cm^{-1}) might also be visible, but in our spectra it is not. We do not have a good explanation for why this is the case, but the behavior of the ν_1 mode is complicated by its near coincidence with $2\nu_2$ ($2 \times 667\ cm^{-1} = 1334\ cm^{-1}$) and the concomitant Fermi resonance (Drago, 1992). It is to be hoped that theoretical modeling will be amenable to solving this problem.

The intensification of the $2\nu_3$ peak may be a general feature of CO_2 interactions with molecules that can hydrogen bond, since it was also observed in H_2S–SO_2–CO_2 ice mixtures (Sandford et al., 1991). Formally 'forbidden' transitions in N_2 (Bernstein and Sandford, 1999) and O_2 (Ehrenfreund et al., 1992) have been observed in H_2O and at least that of N_2 is sensitive to the molecular environment. Similarly, we observe the relative intensity of the 2.135 μm (4684 cm^{-1}) peak to change depending on the conditions (i.e., concentration, temperature, etc.), consistent with it being the CO_2 $2\nu_3$ overtone.

Spectra of frosts vapor deposited at low temperature (such as we have shown here) can differ from those of thick ices made by the cooling of higher temperature materials in a closed cell. It may be that thin films have crystallographic defects that locally break the crystal symmetry making the $2\nu_3$ feature more intense in vapor deposited frosts than it would be in thicker samples annealed in a closed cell. In any case, the intensity of the band is clearly controlled by the abundance of band activator (here H_2O), so, it is a powerful indicator of an H_2O–CO_2 interaction (i.e., of CO_2–H_2O intimate mixing) over at least the five fold concentration range studied here.

Other features enhanced in spectra of our H_2O–CO_2 mixtures relative to those of either pure material include the 2.74 μm (3650 cm^{-1}) and 1.89 μm (∼5300 cm^{-1}) absorptions of H_2O. The 2.74 μm (3650 cm^{-1}) feature is certainly not specific to CO_2, it is known to be caused by other guest molecules in H_2O (Rowland et al., 1991). The 1.89 μm (∼5300 cm^{-1}) peak has appeared previously in published spectra of low temperature amorphous H_2O (Schmitt et al., 1998), and we think it an overtone combination of the aforementioned non-specific 2.74 μm (3650 cm^{-1}) feature with the strong ∼6.3 μm (∼1600 cm^{-1}) bending mode of H_2O. This 1.89 μm peak may be a useful measure of the phase of

the ice, since it diminishes on warming (see Fig. 3 in Schmitt et al., 1998).

During warming of $H_2O/CO_2 = 5$ ices we observe at ~2.70 and ~2.79 μm (3700 and 3590 cm^{-1}) the broad, shifted, peaks of CO_2 in H_2O and also sharper peaks that resemble those of pure CO_2 (see Fig. 5). The results for $CH_3OH/CO_2 = 5$ ices are very similar (see Fig. 7). Although the absorptions seen in Fig. 7 between 2.67 and 2.82 μm (3750–3550 cm^{-1}) look like pure CO_2, they cannot be, both because the temperature is above that at which pure CO_2 would sublime, and also because the corresponding 2.135 μm (4684 cm^{-1}) peak is observed although it is absent from spectra of pure CO_2. Thus, if this CO_2 is 'pure' it is still in small domains, i.e., not a layer of pure CO_2 on top of a layer of pure H_2O. These observations are consistent with previous studies of the temperature dependence of the 4.27 μm (2340 cm^{-1}) CO_2 peak, TEM micrographs (Blake et al., 1991) and the ~15 μm (~650 cm^{-1}) CO_2 peak (Ehrenfreund et al., 1998) in ternary CO_2–H_2O–CH_3OH mixtures. This is reminder that CO_2 can be trapped in H_2O ice at temperatures well above that at which it would normally sublime, so small amounts of solid CO_2 may be observed as long as H_2O ice is present, in our vacuum system up to almost 200 K.

The case of CO_2 in H_2O and CH_3OH exemplifies what is probably a general rule: intermolecular interactions with H_2O will cause significant changes in IR absorptions, so combining spectra of pure materials will not be adequate to reproduce spectra of mixtures. The results reported here have obvious implications for the interpretation of IR spectra of ices in environments where CO_2 might come into contact with H_2O, such as Mars polar caps and outer Solar System objects. Even in environments where one might expect CO_2 to be separate from H_2O because it is more volatile, CO_2 could be formed trapped in solid H_2O by the oxidation of carbon compounds. Since the CO_2 ($2\nu_3$) overtone near 2.134 μm (4685 cm^{-1}) is essentially not present in pure CO_2 but is prominent in mixtures with H_2O, near-IR spectra could be used to determine if, in a Mars polar cap or on the surface of an icy body in the outer Solar System, CO_2 is mixed intimately with another molecule or separate. Since the absorptions of CO_2 in H_2O are broad and thus have lower spectral contrast, they may have been overlooked or assigned to other causes in the past. For example, there is a peak near 2.13 μm on the short wavelength shoulder of the N_2 absorption in the spectrum of Triton presented in Fig. 2 from Quirico et al. (1999) that could be the ($2\nu_3$) overtone of CO_2 in H_2O. The three shorter wavelength CO_2 absorptions (seen in Fig. 4) would be even smaller and thus lost in the noise. However, there is also a nearby shoulder in the lab spectrum of pure N_2 so the presence of this shoulder is merely consistent with some CO_2 in H_2O. It is to be hoped that future observations of Triton, Mars, and other objects where solid H_2O and CO_2 are present will allow for the accurate determination of whether there may be some CO_2 intimately mixed with H_2O.

5. Conclusions

1. We have presented the first near-IR spectra of H_2O/CO_2 and CH_3OH/CO_2 mixtures vapor deposited at 15 K and warmed to 150 K.
2. The spectrum of CO_2 in H_2O is not the same as the sum of the spectra of the pure components. In particular, the 2.135 μm (4684 cm^{-1}) absorption of CO_2 is thousands of times stronger in the mixtures than in pure CO_2.
3. The presence of this absorption in the spectra of Solar System objects will be a good indicator of whether the CO_2 is intimately mixed with H_2O.

Acknowledgments

This work was supported by NASA's Planetary Geology and Geophysics Program (NRA-02-OSS-01-PGG). The authors thank Dr. L.J. Allamandola for helpfull discussions, the expert technical and experimental support of Robert Walker, and Drs. Quirico and Gerakines for helpful comments that improved the manuscript.

References

Bernstein, M.P., Sandford, S.A., 1999. Variations in the strength of the infrared forbidden 2328.2 cm^{-1} fundamental of solid N_2 in binary mixtures. Spectrochim. Acta A 55, 2455–2466.

Bibring, J.-P., Langevin, Y., Poulet, F., Gendrin, A., Gondet, B., Berthé, M., Soufflot, A., Drossart, P., Combes, M., Bellucci, G., Moroz, V., Mangold, N., Schmitt, B., 2004. OMEGA Team, Perennial water ice identified in the south polar cap of Mars. Nature 428, 627–630.

Bini, R., Salvi, P.R., Schettino, V., Jodl, H.-J., 1991. Triphonons in crystal CO_2. Phys. Lett. A 157 (4–5), 273–282.

Blake, D., Allamandola, L.J., Sandford, S.A., Hudgins, D.M., Freund, F., 1991. Clathrate hydrate formation in amorphous cometary ice analogs in Vacuo. Science 254, 548–551.

Buratti, B.J., 28 colleagues, 2005. Cassini VIMS observations of Iapetus: Detection of CO_2. Astrophys. J. 622 (2), L149–L152.

Clark, R.N., 25 colleagues, 2005. Compositional mapping of Saturn's moon Phoebe with Imaging Spectroscopy. Nature. In press.

Cruikshank, D.P., Roush, T.L., Owen, T.C., Geballe, T.R., de Bergh, C., Schmitt, B., Brown, R.H., Bartholomew, M.J., 1993. Ices on the surface of Triton. Science 261, 742–745.

Cruikshank, D.P., 14 colleagues, 1998. The composition of Centaur 5145 Pholus. Icarus 135, 389–407.

Dartois, E., Demyk, K., D'Hendecourt, L., Ehrenfreund, P., 1999. Carbon dioxide–methanol intermolecular complexes in interstellar grain mantles. Astron. Astrophys. 351, 1066–1074.

Drago, R.S., 1992. Physical Methods for Chemists. Harcourt Brace Jovanovich, Fort Worth, TX.

Ehrenfreund, P., Breukers, R., D'Hendecourt, L., Greenberg, J.M., 1992. On the possibility of detecting solid O_2 in interstellar grain mantles. Astron. Astrophys. 260, 431–436.

Ehrenfreund, P., Gerakines, P.A., Schutte, W.A., van Hemert, M.C., van Dishoeck, E.F., 1996. Infrared properties of isolated water ice. Astron. Astrophys. 312, 263–274.

Ehrenfreund, P., Dartois, E., Demyk, E., D'Hendecourt, L., 1998. Ice segregation toward massive protostars. Astron. Astrophys. 339, L17–L20.

Ehrenfreund, P., Kerkhof, O., Schutte, W.A., Boogert, A.C.A., Gerakines, P.A., Dartois, E., D'Hendecourt, L., Tielens, A.G.G.M., van Dishoeck,

E.F., Whittet, D.C.B., 1999. Laboratory studies of thermally processed H_2O–CH_3OH–CO_2 ice mixtures and their astrophysical implications. Astron. Astrophys. 350, 240–253.

Gerakines, P.A., Bray, J.J., Davis, A., Richey, C.R., 2005. The strengths of near-infrared absorption features relevant to interstellar and planetary ices. Astrophys. J. 620, 1140–1150.

Grundy, W.M., Buie, M.W., 2001. Distribution and evolution of CO_2, N_2, and CO ices on Pluto's surface: 1995 to 1998. Icarus 153, 248–263.

Grundy, W.M., Young, L.A., Young, E.F., 2003. Discovery of CO_2 ice and leading–trailing spectral asymmetry on the uranian satellite Ariel. Icarus 162, 222–229.

Hansen, G.B., 1997. The infrared absorption spectrum of carbon dioxide ice from 1.8 to 333 μm. J. Geophys. Res. 102, 21569–21588.

Hibbits, C.A., McCord, T.B., Hansen, G.B., 2000. Distributions of CO_2 and SO_2 on the surface of Callisto. J. Geophys. Res. 105, 22541–22557.

Hibbits, C.A., Pappalardo, R.T., Hansen, G.B., McCord, T.B., 2003. Carbon dioxide on Ganymede. J. Geophys. Res. 108 (E5), 2-1–2-22.

Hudgins, D.M., Sandford, S.A., Allamandola, L.J., Tielens, A.G.G.M., 1994. Mid- and Far-Infrared Spectroscopy of Ices: Optical Constants and Integrated Absorbances. The AAS CD-ROM Series, vol. 1. Expanded version of the tables in Astrophys. J. Suppl. Ser. 86, 713–870.

Jenniskens, P., Blake, D.F., 1994. Structural transitions in amorphous water ice and astrophysical implications. Science 265, 753–756.

Jenniskens, P., Blake, D.F., Wilson, M.A., Pohorille, A., 1995. High-density amorphous ice, the frost on interstellar grains. Astrophys. J. 455, 389–401.

McCord, T.B., 11 colleagues, 1997. Organics and other molecules in the surfaces of Callisto and Ganymede. Science 278, 271–275.

McCord, T.B., 14 colleagues, 1998. Non-water-ice constituents in the surface material of the icy Galilean satellites from the Galileo Near-Infrared Mapping Spectrometer investigation. J. Geophys. Res. 103, 8603–8626.

Mumma, M.J., Weissman, P.R., Stern, S.A., 1993. Comets and the origin of the Solar System: Reading the Rosetta stone. In: Levy, E., Lunine, J. (Eds.), Protostars and Planets III. Univ. of Arizona Press, Tucson, pp. 1177–1252.

Palumbo, M.E., Baratta, G.A., 2000. Infrared spectra of CO_2 in H_2O:CH_3OH:CO_2 icy mixtures. Astron. Astrophys. 361, 298–302.

Quirico, E., Schmitt, B., 1997. Near-infrared spectroscopy of simple hydrocarbons and carbon oxides diluted in solid N_2 and as pure ices: Implications for Triton and Pluto. Icarus 127, 354–378.

Quirico, E., Doute, S., Schmitt, B., de Bergh, C., Cruikshank, D.P., Owen, T.C., Geballe, T.R., Roush, T.L., 1999. Composition, physical state, and distribution of ices at the surface of Triton. Icarus 139, 159–178.

Rowland, B., Fisher, M., Devlin, P.J., 1991. Probing icy surfaces with the dangling OH mode absorption: Large ice clusters and microporous amorphous ice. J. Chem. Phys. 95, 1378–1384.

Roush, T.L., 2001. Physical state of ices in the outer Solar System. J. Geophys. Res. 106 (E12), 33315–33324.

Sandford, S.A., Allamandola, L.J., 1990. The physical and infrared spectral properties of CO_2 in astrophysical ice analogs. Astrophys. J. 355, 357–372.

Sandford, S.A., Salama, F., Allamandola, L.J., Trafton, L.M., Lester, D.F., Ramseyer, T.F., 1991. Laboratory studies of the newly discovered infrared band at 47052 cm^{-1} (2.1253 μm) in the spectrum of Io: The tentative identification of CO_2. Icarus 91, 125–144.

Schmitt, B., de Bergh, C., Festou, M., 1998. Solar System Ices. Astrophysics and Space Science Library (ASSL) Series, vol. 227. Kluwer Academic, Dordrecht, p. 826.

Stansberry, J.A., 2004. Triton, Pluto, and beyond. In: Dasch, F. (Ed.), Icy Worlds of the Solar System. Cambridge Univ. Press, Cambridge, UK, pp. 139–167.